Photonic Curing of Silver Nanoparticle Based Inks

J. West[*], M. Carter[**], S. Smith[*] and J. Sears[**]

[*]Nanoscience and Nanoengineering, South Dakota School of Mines and Technology, Rapid City, SD, USA, Steve.Smith@sdsmt.edu
[**]Additive Manufacturing Laboratory, Rapid City, SD, USA, James.Sears@sdsmt.edu

ABSTRACT

Photonic Curing is a method of sintering nanoparticle based films using a high intensity, short (<1 ms) pulse of light from a xenon flash lamp. By measuring the amount of densification produced by the flash lamp at various pulse durations and lamp voltages, the optimal conditions for curing silver films were obtained. The absorption spectrum of the silver films was calculated using Bruggeman's effective medium theory, and compared with the measured absorption spectrum acquired using a UV-Vis spectrophotometer. Simulations of the temperature profile of the silver nanoparticle films were made using the fluid dynamics simulation program Fluent™. The simulations indicate that the nanoparticles melt during the photonic curing process, and then rapidly cool to room temperature, as is observed in experiments.

Keywords: photonic curing, xenon flash lamp, light absorption, Bruggeman's theory, Fluent simulations

1 INTRODUCTION

Photonic Curing is a low thermal exposure sintering method developed to functionalize deposited nanoparticle thin films. Photonic Curing was developed by Nanotechnologies (now NovaCentrix) of Austin, Texas, and first made public in 2006 [1]. The technology sinters the nanoparticles without significantly raising the temperature of the substrate. This is accomplished through use of a xenon flash lamp. There are two main parameters that control the amount of sintering from the flash lamp; the duration of the light pulse and the intensity of the lamp. The flash lamp is suspended above the deposition and a current pulse is run through the flash lamp. The current causes the xenon flash lamp to issue a high intensity, broad spectrum pulse of light. This pulse of light is absorbed by the nanoparticles, heating them to such a degree that they fuse to form a continuous film.

One of the primary advantages of this method is that the high intensity pulse of light produces minimal damage to low temperature substrates, much less than oven or laser sintering [2]. This allows the nanoparticles to be deposited and cured on a large variety of low temperature substrates such as cloth, paper, and Mylar. Another advantage of using photonic curing is the speed at which nanoparticle depositions can be sintered. Rather than spending hours in an oven or programming a laser to follow the deposition path, the photonic curing process can sinter large areas (~ 200 cm^2 per 10 cm long lamp) in < 2 ms. The sintered depositions can be tailored for use in flexible circuit boards, RFID tags, or flat panel displays [2].

Three basic assumptions were considered during the development of Photonic Curing for sintering nanoparticles; (i) nanoparticles are predominantly black, they should therefore strongly absorb light; (ii) once light is absorbed by the nanoparticles, due to their high surface area to mass ratio, the nanoparticles should heat easily and sinter quickly; and (iii) as nanoparticle films are very thin, they should not retain heat very well and therefore should cool rapidly, minimizing damage to the substrate [1]. Photonic curing has been shown to sinter conductive nanoparticle metals (*e.g.*, silver, gold and copper) as well as dielectric nanoparticles made of alumina, zirconia, barium titanate, and mica, as well as the soft magnetic materials cobalt ferrite and iron-nickel permalloy [2].

2 EXPERIMENTAL RESULTS

Test specimens consisting of printed lines of nanoparticle silver were deposited onto low temperature substrates and photonically cured. The densification and optical absorption of these films were measured for varied photonic curing conditions in order to optimize the process. Densification was determined by measuring the film thickness before and after curing and the optical absorption was measured using a UV-Vis spectrometer on un-sintered depositions of similar thickness to the deposited lines.

2.1 Densification

To observe the volume shrinkage that occurs during photonic curing, a Zeiss Imager M1M microscope was used to determine the focal length at the surface of the deposition prior to and after curing, using the microscopes 3-D imaging software. The silver nanoparticles were deposited in lines 3 mm x 10 mm, with an average thickness of 4.7 μm. The samples were weighed and compared with the mass of a blank slide to obtain the mass of the deposition. Using this procedure, we calculate a silver density for these depositions of 3.8 g/cm^3. Knowing the mass of the total deposition, size of the silver nanoparticles, density of bulk silver, and volume of the deposition, allows the calculation of the volume density of the silver nanoparticles. The volume fraction of silver nanoparticles in these depositions was found to be 36%.

The thickness of these depositions after photonic curing at various lamp voltages and pulse durations, were measured. The densification of the deposition was then calculated and the results are shown in Figure 1. Significant volume shrinkage occurred at higher intensities and longer pulse lengths. The volume shrinkage was dependent on how much voltage was applied to the flash lamp and the duration of the pulse. However, the depositions were damaged if the flash lamp voltage was set greater than 1600 volts.

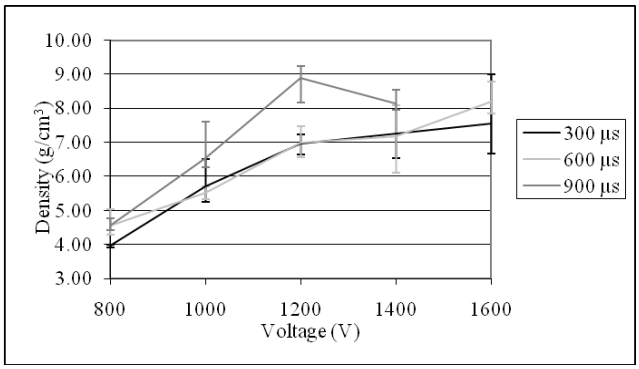

Figure 1: Density vs. flash lamp voltage for three pulse lengths. The density of bulk silver is 10.6 g/cm^3.

2.2 Absorption

To characterize the absorption of the silver nano-ink depositions, a UV-Vis spectrometer was used to measure the absorption of the uncured depositions. The silver nanoparticles were deposited in 1 cm x 1 cm squares at operational deposition thickness, verified using the Zeiss optical microscope. The UV-Vis spectrometer measures the absorbance every 2 nm in wavelength, from 190 nm to 820 nm. The absorption percentages for two sample thicknesses are shown in Figure 2. These measurements show significant absorption over a broad spectrum.

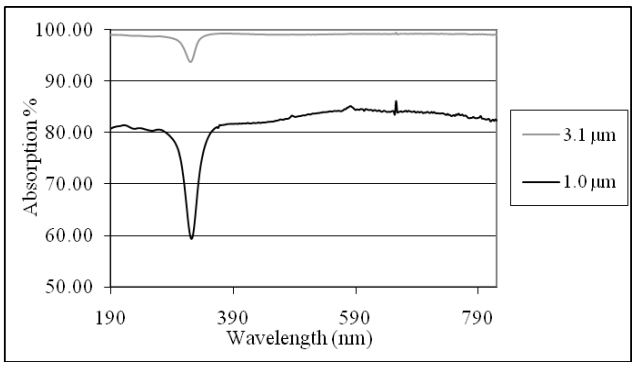

Figure 2: Absorption spectrum for two thicknesses of the silver film.

3 SIMULATION RESULTS

The absorption and scattering of metallic nanoparticle-based inks is the result of multiple physical mechanisms that contribute to the total absorption. We calculated the contribution due to the metallic nanoparticles themselves using the effective medium theory of Bruggeman. From these simulations we show that Bruggeman's effective medium theory, using published optical constants, reproduces the spectral dependence of the absorption of these films.

The heat equation was solved for a slab of metal-nanoparticle composite, in contact with air on the irradiated face and conductively cooled by the substrate on the opposite face, in order to simulate the heating and melting processes that occur during photonic curing. These simulations place constraints on the photonic curing process, based on heat transfer and thermodynamics. Our simulations reproduce the very fast sintering of the metallic nanoparticle-based inks observed in the laboratory, and suggest that traditional sintering models do not apply to photonic curing. Such simulations may act as a guide in designing deposition and photonic curing processes.

3.1 Bruggeman Model

An effective medium theory, due to Bruggeman, was found to accurately predict the absorption of Ag nanoparticle films [3]. In such a theory, the average dielectric function of an inhomogeneous medium is found by averaging the dielectric function of the medium's constituents, taking into account their respective volume fraction in the medium. The most popular effective medium theories are the Maxwell Garnett theory and the Bruggeman theory. Research has shown that the Maxwell Garnett theory breaks down with high volume fractions of material suspended within the medium [4-6], while the Bruggeman dielectric function has been shown to work well with higher volume fractions [3, 4]. The Bruggeman dielectric function is defined by the expression:

$$f\frac{\varepsilon-\varepsilon_{AV}}{\varepsilon+2\varepsilon_{AV}}+(1-f)\frac{\varepsilon_m-\varepsilon_{AV}}{\varepsilon_m+2\varepsilon_{AV}}=0 \qquad (1)$$

where ε is the dielectric function of the particles in the medium, ε_m is the dielectric function of the medium, ε_{AV} is the average dielectric function, and *f* is the volume fraction of the particles contained in the medium [4]. Once the average dielectric function is found, after calculating the imaginary portion of the refractive index, the absorption coefficient for the effective medium can be calculated by the expression:

$$\alpha' = \frac{4\pi k}{\lambda} \qquad (2)$$

where k is the imaginary part of the refractive index and λ is the wavelength of light [7]. From this, using the Beer-Lambert law [7], the absorption spectra was calculated. A graph comparing the absorption results using Bruggeman's theory with the measured absorption is shown in Figure 3. While the spectral dependence of these spectra is in good agreement, the magnitude of the absorption from the theory was much larger than the measured spectra of the same thickness.

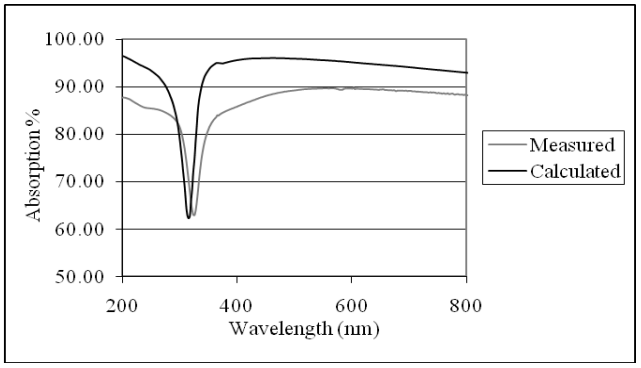

Figure 3: Comparison of the simulated absorption using Bruggeman's theory with a thickness of 150 nm with the measured absorption using thickness of 1.3 μm.

3.2 Heat Equation Simulations

To model the sintering of the silver nanoparticle film, we solved the heat equation under the conditions of radiative heating from the top surface, convective cooling of the top surface, and conductive cooling from the bottom surface, using the relevant solvers built into the fluid dynamics and heat transfer modeling package Fluent™. The results give the simulated temperature that the nanoparticles reached as a result of the photonic curing process as a function of time. These two properties are fundamental in understanding the solid state sintering process [8, 9]. Using this software allowed us to model the temperature profile of a silver nanoparticle film during the photonic curing process, the amount of time the film took to cool, the progression of the melting of the film, and the effect of different deposition substrates upon the film temperature. These simulations can help explain how the silver nanoparticle films are sintered so rapidly and completely and may be used as a guide to predict the optimum settings for the photonic curing system.

Fluent is a computational fluid dynamics program that uses the finite volume method on a grid to calculate fluid flow, acoustics, and combustion. Fluent also has heat transfer, phase change, and radiation models, which are the models that were used for this work. A 10 μm x 100 μm x 100 μm volume was created for the simulations. The top surface of the slab was set to undergo convective cooling by air along with radiative heating by the light from the flash lamp. The sides of the slab were convectively cooled by the air and the bottom of the slab was set to be conductively cooled by a glass substrate. In order to simulate the radiative heating Fluent asks for the external radiation temperature and the external emissivity to be input. The external emissivity was taken from earlier experimental measurements and set to 0.99 for the 10 μm thick slab, meaning that virtually all of the radiation would be absorbed by the slab. The external radiation temperature was found using Stefan's law [10].

To simulate convective cooling Fluent needs the temperature of the air far from the slab and the heat transfer coefficient for the air. The temperature of the air far from the slab was set to 294 K. Calculating the heat transfer coefficient was done using the Nusselt number. However, the Nusselt number first had to be calculated from the Rayleigh number and the Prandtl number. The Prandtl number is defined as:

$$\mathrm{Pr}_x = \frac{c_p \mu}{k} \tag{3}$$

where c_p is the specific heat, μ is the dynamic viscosity, and k is the thermal conductivity [11]. The Prandtl number is evaluated at the film temperature, which was estimated as:

$$T_f = \frac{T_w - T_\infty}{2} \tag{4}$$

where T_w is the temperature of the wall and T_∞ is the temperature far from the wall [11]. After finding the Prandtl number the Rayleigh number can be found by multiplying the Prandtl number by the Grashof number, $Ra_x = Gr_x * \mathrm{Pr}$ [11]. The Grashof number for a heated vertical flat plate is:

$$Gr_x = \frac{g\beta(T_w - T_\infty)x^3}{\nu^2} \tag{5}$$

where g is the gravitational constant, β is the coefficient of volumetric expansion, x is the characteristic length, and ν is the kinematic viscosity [11]. For an ideal gas the coefficient of volumetric expansion is $\beta = 1/T_f$ [11]. The Grashof number was also evaluated at the film temperature. With these values for the Rayleigh and Prandtl numbers, the Nusselt number for free convection at a vertical wall is calculated as:

$$Nu_x = 0.68 + \frac{0.67 Ra_x^{1/4}}{\left[1 + (0.492/\mathrm{Pr}_x)^{9/16}\right]^{4/9}} \tag{6}$$

for Rayleigh numbers less than 10^9 [11]. After calculating the Nusselt number the heat transfer coefficient can be found from

$$h = \frac{Nu_x k}{x} \tag{7}$$

using the thermal conductivity at the film temperature [11]. In Fluent™ the heat transfer coefficient can only be input as a single value. To find a heat transfer coefficient that would affect the simulation for the longest period of time, a heat transfer coefficient of 3500 was used which corresponds to a slab temperature of 834 °C.

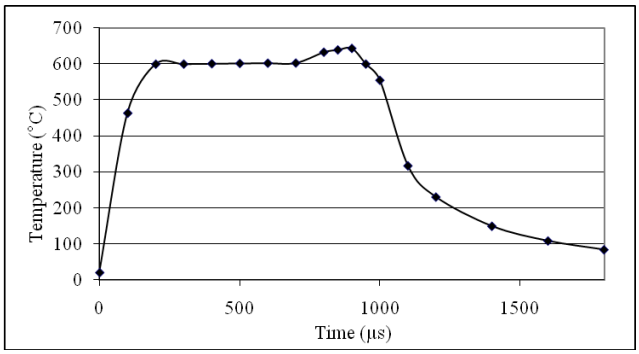

Figure 4: Simulated temperature vs. time of a 900 μs pulse using a flash lamp voltage of 1200V on a 10 μm thick deposition of silver nanoparticles.

The convective cooling model in Fluent uses the thermal conductivity, specific heat, and density of the glass, Mylar, and Kapton substrates. The interior of the slab was specified to be a porous medium containing 33% silver and 67% air to correspond to the volume densities previously measured. The properties of the silver that Fluent required were the density, thermal conductivity, specific heat, melting heat, viscosity, solidus temperature, and liquidus temperature. The thermal conductivity was set to change with the temperature. The solidus and liquidus temperatures were set to 600 °C, which is the temperature the V2 ink has been observed to melt at. A graph of the temperature vs. time is shown in Figure 4. The simulations indicated that the deposition rapidly heated to the melting point and melted during the curing process. Following the end of the pulsed irradiation, the deposition quickly solidified and cooled to room temperature. These results suggest that traditional solid state sintering models do not apply to photonic curing, as in solid state sintering the temperatures applied do not melt the materials, and the heat is applied over a long period of time, allowing diffusive mass transport [8, 9].

4 CONCLUSIONS

In examining the photonic curing process, a number of interesting results were found. It was shown that there is significant densification of the photonically cured silver, with the photonically cured silver reaching 84% of the density of bulk silver. In measuring light absorption in uncured silver nanoparticle films it was observed that the absorption is broadband, and the plasmon resonance is not the dominating feature of this absorption. The Bruggeman effective medium model was shown to approximate the absorption for the silver nanoparticle ink. Results using the Fluent™ fluid dynamics and heat transfer modeling package indicated that the silver depositions melted during the photonic curing process, which suggests that solid state sintering models do not apply to photonic curing.

REFERENCES

[1] K. A. Schroder, S. C. McCool and W. R. Furlan, Technical Proceedings of the 2006 NSTI Nanotechnology Conference and Trade Show, 3, 198-201, 2006.

[2] M. Carter, J. Sears, Advances in Powder Metallurgy & Particulate Materials – 2007: Proceedings of the 2007 International Conference on Powder Metallurgy & Particulate Materials, May 13-16, Denver, Colorado, 2007.

[3] D. A. G. Bruggeman, Ann. Phys. (Leipzig), 24, 636-679, 1935.

[4] C. F. Bohren and D. R. Huffman, "Absorption and Scattering of Light by Small Particles," New York: John Wiley & Sons, Inc., 1983.

[5] J. C. Maxwell Garnett, Philos. Trans. R. Soc., A203, 385-420, 1904.

[6] A. Garahan, L. Pilon, J. Yin and I. Saxena, Journal of Applied Physics, 101, 014320, 2007.

[7] D. Skoog, F. J. Holler and T. Nieman, "Principles of Instrumental Analysis," Thompson Learning, 1998.

[8] R. M. German, "Sintering Theory and Practice," New York: John Wiley & Sons, Inc., 1996.

[9] S. L. Kang, "Sintering: Densification, Grain Growth, and Microstructure," Oxford: Elsevier Butterworth-Heinemann, 2005.

[10] R. Eisberg and R. Resnick, "Quantum Physics of Atoms, Molecules, Solids, Nuclei, and Particles," New York: John Wiley & Sons, Inc., 1974.

[11] F. W. Schmidt, R. E. Henderson and C. H. Wolgemuth, "Introduction to Thermal Sciences," New York: John Wiley & Sons, Inc., 1984.